Article

On-Line Wavelets Filtering with Application to Linear Dynamic Data Reconciliation

Hsiao-Ping Huang, and Kuo-Yuan Luo

Ind. Eng. Chem. Res., **2007**, 46 (25), 8746-8755 • DOI: 10.1021/ie061410k

PROCESS DESIGN AND CONTROL

On-Line Wavelets Filtering with Application to Linear Dynamic Data Reconciliation

Hsiao-Ping Huang* and Kuo-Yuan Luo

Department of Chemical Engineering, National Taiwan University, Taipei 10617, Taiwan, Republic of China

An on-line robust wavelet filtering is presented and applied to the dynamic data reconciliation problem via a constrained Kalman filter approach. The wavelet filtering is used to remove outliers and provide data smoothing prior to the reconciliation. Matrix computation is presented to facilitate the implementation of discrete wavelet transform (DWT) and inverse discrete wavelet transform (IDWT) for on-line filtering. An endpoint correction method is presented to overcome the endpoint effect that is caused by wavelet filtering on an on-line moving data window. The filtered outputs are treated as the output measurements in the subsequent Kalman filter estimations. This latter filter is to estimate the state variables, subject to both dynamic and static equality constraints. Using accumulative balancing constraints, a method is proposed to detect and isolate the existence of single gross error in a dynamic system. A simulated example is used to illustrate the use and performance of this proposed dynamic data reconciliation method.

1. Introduction

In a dynamic process, process variables are constrained by both differential and algebraic equations. Measurements of these process variables are prone to be contaminated by noises. Therefore, data reconciliation is useful to procure accurate and consistent data from measurements for purposes such as material/energy balances, and control. In the context of state estimations, Kalman filtering is useful to estimate the states of a dynamic system from its measured outputs. In this capacity, it has been used in the problems of dynamic data reconciliation. Applications of the Kalman filter approach to the dynamic data reconciliation have been reported in the literature.[1−5] The reason why Kalman filtering prevails is that it provides minimum-variance estimations for the state variables in a dynamic way and has a recursive formulation, which is suitable for online implementation, provided that all these process variables to be reconciled are observable from its measured outputs. It was mentioned in the book by Narasimhan and Jordache[6] that such Kalman filter estimations are identical to problems of steady-state data reconciliation. In the application of Kalman filter for data reconciliation, two major difficulties may be encountered. First, the original formulation of the Kalman filter does not consider equality constraints. Second, not all the process variables to be reconciled are state variables in the representation of system dynamics. To overcome the first difficulty, some late works[7−9] have provided theoretical bases to incorporate equality constraints and, thus, can be used for this purpose. To overcome the second difficulty mentioned, variables originally not in the list of state variables can be augmented as new state variables. By doing so, measurement errors in these variables will be carried over to become state uncertainties. Thus, filtering the data to reduce these uncertainties due to measurement noises becomes desirable and is one of the objectives of this research.

Generally, linear filters such as mean filter, exponential filter, and the exponentially weighted moving average (EWMA) filter, etc., are easier for on-line uses. In these cases, the tuning parameters in the filters are essential for their performances. One common drawback among these filters is that they are not capable of removing data outliers. To remove non-Gaussian outliers, nonlinear filters such as the mean filter and the FIR−median hybrid (FMH) filter[10] have been used. In the application of such nonlinear filters, tradeoffs between performance and filter length or computation efforts always must be made. The aforementioned nonlinear filters are good for preserving sharp changes in the data and removing the outliers. They are most suitable for off-line uses and have difficulties for on-line applications. As illustrated in Figure 1, the filter removes outliers only in one direction. This fact is attributed to those virtual data beyond the endpoint being taken as zero.

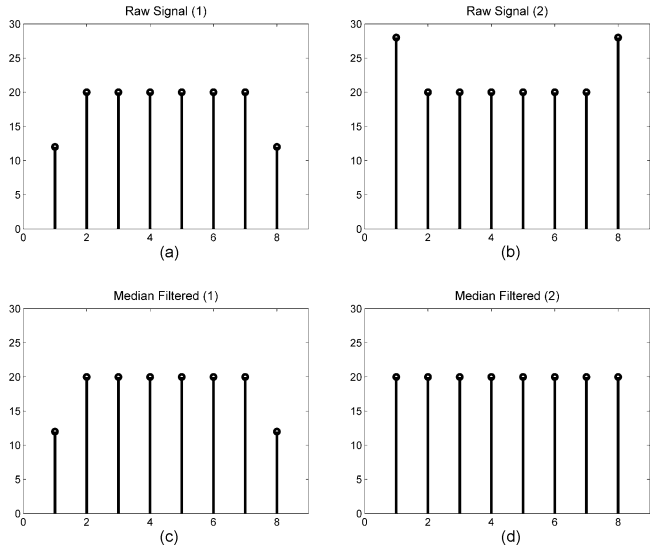

Figure 1. Performance of the median filtering: (a) raw signal 1, (b) raw signal 2, (c) the median filtered result of signal 1, and (d) the median filtered result of signal 2.

Motivated by the aforementioned difficulties, a new approach is proposed for dynamic data reconciliation. In this approach, a

* To whom correspondence should be addressed. Tel.: +886-2-2363-8999. Fax: +886-2-2362-3935. E-mail address: huanghpc@ntu.edu.tw.

10.1021/ie061410k CCC: $37.00
Published on Web 11/03/2007

robust wavelet filtering method is proposed to prefilter the data and remove possible outliers. In this prefiltering approach, the DWT and IDWT algorithm is adopted.[11] An algorithm is proposed to correct the possible outliers in the measurement. A wavelet filtering method based on the concepts of "Translation Invariant" and "Boundary Correction" is proposed to enhance its performance and robustness. Then, a reformulated Kalman filter is used to estimate the state variables and detect constant biased gross errors in the data. The advantages of this presented method include (i) a new way to overcome the difficulty encountered in applying wavelet for filtering data in a short moving data window, which is required for on-line implementation, and (ii) a new reformulated constrained Kalman filter for reconciling estimations and to detect gross error by checking the estimation results with accumulative balancing constraints. Finally, a storage-tank process is used to illustrate the performances of the proposed method.

2. Filtering by Wavelets

Recently, wavelet analysis has been a useful tool for data filtering. The principle behind filtering is to perform a threshold step on the corresponding coefficients obtained from a wavelet analysis and reconstruct the thresholded coefficients via an inverse transformation. Several threshold methods, such as Hard shrink, Soft shrink, VisuShrink, and SureShrink, to name a few,[12−14] have been reported in the literature. These methods have a tendency to restore spurious features near large changes in the measurement data. Corrections to those spurious features have also been proposed by some researchers,[15,16] using the so-called "Translation Invariant" concepts. For on-line applications, one inherent weakness of this filter is the need for future data in computation. Methods to pad known data points (e.g., periodic padding, mirroring padding, etc) or to design boundary filters are presented to overcome this difficulty.[17] However, these padding approaches do not work in cases where the data have outliers. Nounou and Bakshi[18] combined the use of the "VisuShrink" threshold method and the multi-scale median method of Bruce et al.[19] for filtering. This method is good for filtering Gaussian noises, single outliers, and outlier patches. However, it demands a maximum available dyadic length, which results in huge computation burdens. Moreover, it has the same drawback that the median method has. In fact, the method of Bruce et al.[19] was originally proposed for outlier removal in off-line and batch filtering. Doymaz et al.[20] also presented a robust filtering methodology through a combination of median filtering and the wavelet "WienerShrink" approach. However, the boundary problem is not considered in their approach.

In the following, in terms of matrix algebra, a quick computation formula for filtering and a method to achieve the filtering robustness in dealing with the endpoint effect will be presented.

2.1. DWT and IDWT Analysis for Filtering. The wavelets analysis is known as a multiresolution analysis (MRA), which divides the frequency contents of a signal into low and high sub-bands. In practice, DWT and IDWT involve a pyramidal algorithm based on convolutions with corresponding FIR filters.[11] Based on Mallat's algorithm, DWT and IDWT can also be expressed in the matrix form:[17]

$$\mathbf{c} = \mathbf{T}_a\mathbf{y} \tag{1}$$

$$\mathbf{y} = \mathbf{T}_s\mathbf{c} \tag{2}$$

where $\mathbf{c}$ is a matrix that consists of coefficients from several high-pass bands and one low-pass band, $\mathbf{y}$ is the raw signal, $\mathbf{T}_a$ is the decomposition matrix, and $\mathbf{T}_s$ is the reconstruction matrix. In $\mathbf{c}$, all the DWT coefficients are included, up to a prescribed analysis level. The thresholding methods are those which screen $\mathbf{c}$ to be used in eq 2 for reconstruction. For dynamic data reconciliation, generally, the low-pass signals are more meaningful for material/energy balances than the high-frequency signals. Consequently, only part of $\mathbf{c}$ will be used for reconstruction. Thus, Mallat's pyramidal algorithm can be expressed as eq 3 if only the low-pass coefficients of analysis level j are kept:

$$\mathbf{y}^{(j)} = \underline{\mathbf{S}}_1\underline{\mathbf{S}}_2 \cdots \underline{\mathbf{S}}_j\underline{\mathbf{T}}_j \cdots \underline{\mathbf{T}}_2\underline{\mathbf{T}}_1\mathbf{y} = \Lambda_j\mathbf{y} \tag{3}$$

where $\underline{\mathbf{T}}_j$ and $\underline{\mathbf{S}}_j$ are decomposition and reconstruction matrices, respectively. In eq 3, $\mathbf{y}^{(j)}$ is the approximate or filtered signal, of which only the low-pass coefficients up to level j are kept. Determination of the level (i.e., j) for analysis will be given later. With the adopted padding strategy (in this paper, constant padding is adopted), $\underline{\mathbf{T}}_j$ and $\underline{\mathbf{S}}_j$ are given in the Appendix. Notice that matrix $\underline{\mathbf{T}}_j$ is used to generate the jth-level low-pass coefficients ($\boldsymbol{\lambda}_j$) from the $(j-1)$th-level coefficients ($\boldsymbol{\lambda}_{j-1}$) using the following relationship:

$$\boldsymbol{\lambda}_j = \underline{\mathbf{T}}_j\boldsymbol{\lambda}_{j-1} \tag{4}$$

Let k denote the length of a moving data window. According to eq 3, $y_k^{(j)}$ is given by multiplying the last row of Λ_j by $\mathbf{y}$:

$$y_k^{(j)}(t) = \Lambda_j(k,:)\mathbf{y}(t) \tag{5}$$

Notice that $y_k^{(j)}$ is the filtered output from the current moving data window along the current time t.

2.2. Determining the Wavelets Filtering Level. To preserve the low-frequency contents in the signal after filtering, one must set a proper number for the analysis level j, so that detail portions up to this jth level are removed. The remaining low-pass signal is designated as $\mathbf{y}^{(j)}$. In a previous work, Huang and Luo[21] proposed this j value as the level below that where removal of the next higher portion causes a sudden increase in the mean of the high-pass errors. This is because a sudden increase in the mean values from the removal of the high-pass portion at level $j+1$ means that some significant low-frequency signal components are included in that discarded portion and should be avoided. This method requires some modification to address a moving window for on-line application. The modification is to incorporate a Student t-test and a χ^2 hypothetical test, in addition to the MSE on the residuals of the filtered signals at different levels. The residual, $\mathbf{d}^{(j)}$ at the jth level is defined as

$$\mathbf{d}^{(j)} = \mathbf{y} - \mathbf{y}^{(j)} \tag{6}$$

The Student t-variable and the χ^2 variable for a certain level j are defined in eqs 7 and 8:

$$t^{(j)} = \frac{\bar{\mathbf{d}}^{(j)}}{s_d^{(j)}/\sqrt{k+1}} \tag{7}$$

$$\chi^{2,(j)} = \frac{\mathbf{d}^{(j)^{\mathrm{T}}}\mathbf{d}^{(j)}}{s_d^{(j)2}} \tag{8}$$

where $s_d^{(j)}$ is the standard deviation of $\mathbf{d}^{(j)}$ and is obtained from eq 9.

$$s_d^{(j)} = \frac{\sqrt{\sum_{i=1}^{k} (d_i^{(j)} - \bar{\mathbf{d}}^{(j)^2})}}{k-1} \tag{9}$$

The desired number j, which is designated as j^*, is determined by the following:

$$j^* = \text{Arg}\max_j \{\mathbf{d}^{(j)^T}\mathbf{d}^{(j)} = \chi^{2,(j)} s_d^{(j)2} \mid \chi^{2,(j)} < c_{1-\alpha_1}(\nu) \text{ and } t^{(j)} < \eta_{1-\alpha_2}\} \tag{10}$$

where $c_{1-\alpha_1}(\nu)$ is the value of χ^2, which has ν degrees of freedom at a confidence level α_1. The constant η is the value of the Student t-variable at a confidence level of α_2. The Student t-variable and the χ^2 variable are used to ensure that both the mean and the variance of the residuals are normally distributed after the filtering.

2.3. Robust Wavelet Filtering Method. The proposed on-line wavelet filtering method starts with an initial data window. The median filtering is applied to the data in this initializing data window to ensure that there is no obvious outlier in this window. Whenever the window moves, a preconditioning step is taken. The preconditioning step is to make correction to the new measurement via the following:

$$y_k(t) = \hat{y}_k(t-1) + 3 \times \text{sign}(y_k(t) - \hat{y}_k(t-1)) \times s_d \quad (\text{if } |y_k(t) - \hat{y}_k(t-1)| > 3s_d) \tag{11}$$

where $\hat{y}_k(t-1)$ designates the last filtered data from the previous window, $y_k(t)$ is the latest raw data adopted into the window at current time t, and s_d is the variance of the signal in the data window. Estimation of the term s_d is discussed in next section. Equation 11 is used to correct the suspected outlier measurements.

After finishing the preconditioning step to this new data window, eq 5 is applied to this new window to give a filtered output at the current time t. Since padding data are used in the implementation of DWT, the filter output thus obtained is prone to have greater distortion. This distortion is known as the end-point effect, which primarily affects the on-line filtering result. Correction to this distortion to improve the filtering robustness is the main purpose here. As shown in Figure 2, after having the preconditioned data window, several translation windows are generated by performing cycle-spinning on a section of data in this preconditioned data window. Then, to each of the translation windows, eq 5 is applied, to obtain its provisional output. This provisional output then is used to update and apply eq 5 on the translation window iteratively until it converges. Finally, an averaged value of all converged filtered outputs from all the translated widows is taken as the final output at time t. The procedures are illustrated in the block diagram shown in Figure 3. When window moves on, the filtered output is generated sequentially with the aforementioned procedures, along with the window moves.

2.4. Illustrative Examples. 2.4.1. Example 1. Consider filtering a Havisine signal, using Nounou and Bakshi's approach[18] for comparison. The lengths of the moving window and the median filter used in the Nounon and Bakshi's method[18] are set as 1024 and 15, respectively. Furthermore, the analysis depth is set as 6 and a Daubechies wavelet with an order of 2 is adopted. On the other hand, for the proposed method, the length of the moving window is taken as 64, the length of the translations is 20, and a Daubechies wavelet with an order of 6 is adopted. In both cases, 1024 data points are collected from the simulation. The filtering results of the two approaches are compared by calculating their MSE values. Using Nounou and Bakshi's approach,[18] the resulting MSE is 0.1314. On the other hand, the MSE that resulted from the proposed approach is 0.0623. The results of the data are illustrated in Figure 4.

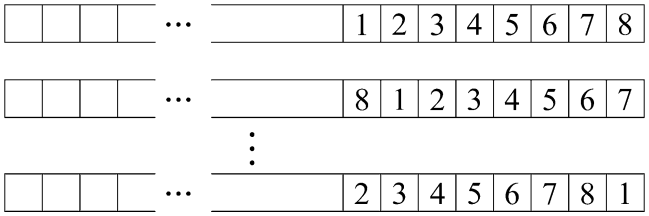

Figure 2. Translation of the data points near the end of the data window.

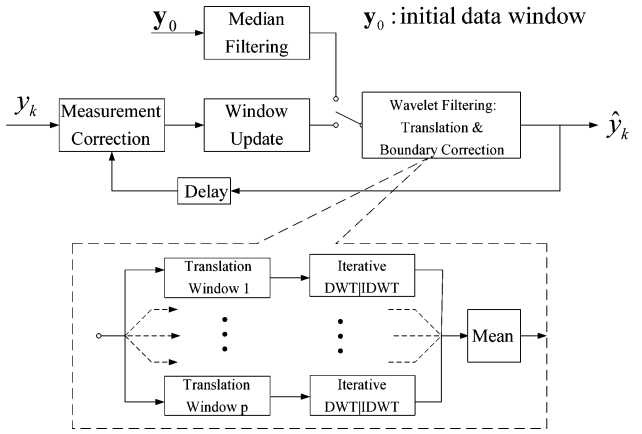

Figure 3. Illustration of the proposed robust filtering approach.

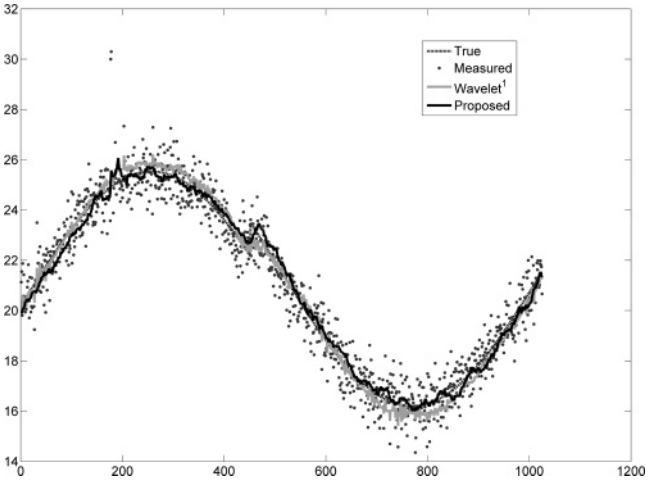

Figure 4. Filtering result of the two approaches. Mean-square-error (MSE) values: wavelet, 0.1314; proposed, 0.0623. (The term "wavelet" denotes the approach by Nounou and Bakshi.[18])

2.4.2. Example 2. Again, consider the same Havisine signal that has a patch of outliers. The colored noise is used besides the patch of the outliers. The colored noise is generated by the autoregressive noise model with the form $e_t = 0.5(e_{t-1} + a_t)$. The white noise (a_t) has a variance of 0.2. Using Nounou and Bakshi's approach,[18] the length of the moving window is set to 1024, the length of the median filter is set to 29, the number of analysis level is set to 6, and a Daubechies wavelet with an order of 2 is adopted. For the proposed method, the length of the moving window is set to 32, the length of the translations is set to 12, and a Daubechies wavelet with an order of 6 is adopted. The results are illustrated in Figure 5. From the illustration, an unfavorable performance occurs because of the patch of outliers in Nounou and Bakshi's approach.[18]

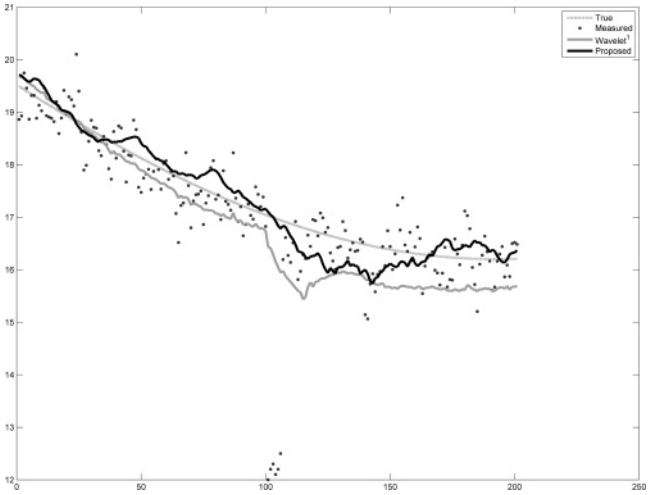

Figure 5. Filtering result of the two approaches.

3. Data Reconciliation with a Moving Data Window

Recently, Simon and Chia[9] has reported a constrained Kalman filter approach for dynamic systems that has equality constraints on state variables. The state-constrained problem was also discussed by Porrill[7] and Hayward,[8] where the perfect measurement approach was considered. To apply the constrained Kalman filter for on-line data reconciliation, each moving data window that contains raw measurements is updated by its latest measurements. The wavelet filtering is then applied to each data window to generate wavelet−filter outputs. The wavelet filtering outputs serve as the measurement outputs in the Kalman filter estimation. With previously estimated values of state as initial values, the Kalman filter with equality constraints computes the next new estimated state. The procedures are repeated as the new raw measurements become available.

3.1. Data Reconciliation Using the Constrained Kalman Filter Approach. The constrained Kalman filter approach of Simon and Chia[9] is adopted as the theoretical basis here for formulating the reconciliation. The solution to this constrained estimation problem consists of two steps. First, an unconstrained estimation is computed; then, the estimation is corrected. The unconstrained Kalman filter solution can be found in some text books (e.g., see the work of Grewal and Andrews[22]).

Consider a time-invariant system with the following constraints:

$$\dot{\mathbf{x}}_a = \mathbf{A}\mathbf{x}_a + \mathbf{B}\mathbf{x}_b + \mathbf{w}_a \tag{12}$$

$$\mathbf{Y} = \begin{bmatrix} \mathbf{C}_a & 0 \\ 0 & \mathbf{C}_b \end{bmatrix} \begin{bmatrix} \mathbf{x}_a \\ \mathbf{x}_b \end{bmatrix} + \mathbf{e} \tag{13}$$

$$\mathbf{D}\begin{bmatrix} \mathbf{x}_a \\ \mathbf{x}_b \end{bmatrix} = \mathbf{d} \quad \text{or} \quad \mathbf{DE}\begin{bmatrix} \mathbf{x}_a \\ \mathbf{x}_b \end{bmatrix} = \mathbf{d} \tag{14}$$

where $\mathbf{x}_a$ and $\mathbf{x}_b$ are vectors of the state and input variables, respectively. $\mathbf{Y}$ ($\mathbf{Y} = [Y_1\ Y_2\ \cdots]$) is a vector of measurement outputs. The system noise ($\mathbf{w}_a$) and measurement noise ($\mathbf{e}$) are assumed to have covariance matrices $\mathbf{Q}_a$ and $\mathbf{R}$. For the reconciliation application, the aforementioned system is reformulated to the augmented state system as

$$\begin{bmatrix} \dot{\mathbf{x}}_a \\ \dot{\mathbf{x}}_b \end{bmatrix} = \begin{bmatrix} \mathbf{A} & \mathbf{B} \\ 0 & 0 \end{bmatrix} \begin{bmatrix} \mathbf{x}_a \\ \mathbf{x}_b \end{bmatrix} + \begin{bmatrix} \mathbf{w}_a \\ \mathbf{w}_b \end{bmatrix} \tag{15}$$

where $\mathbf{w}_b$ is assumed to have a variance matrix $\mathbf{Q}_b$. In the reconciliation problem, $\mathbf{C}_a$ and $\mathbf{C}_b$ are identity matrices. The reformulated matrix $\mathbf{Q}$, as system noise, is then equal to

$$\mathbf{Q} = \begin{bmatrix} \mathbf{Q}_a & \\ & \mathbf{Q}_\mathrm{b} \end{bmatrix} \tag{16}$$

The constrained estimations are obtained by the following equation:

$$\tilde{X} = \hat{X} - P\mathbf{D}^\mathrm{T}(\mathbf{D}P\mathbf{D}^\mathrm{T})^{-1}(\mathbf{D}\hat{X} - \mathbf{d}) \tag{17}$$

where $X = [\mathbf{x}_a\ \mathbf{x}_b]^\mathrm{T}$, $\hat{X}$ is the estimation of the augmented state vector without considering the constrains, and P is the covariance matrix of the state estimations.

The standard deviation for each raw measured variable (s_{Y_i}) can be roughly estimated by applying eq 18 to each measurement Y_i in the moving data window:

$$s_{Y_i}^{\ 2} = \xi \frac{\sum_{p=1}^{k} (y_{i,p} - y_{i,p}^{(j)})^2}{k-1} \tag{18}$$

where $y_{i,p}$ is the pth measurement in the data window of Y_i, $y_{i,p}^{(j)}$ is the corresponding wavelets filtered value, and ξ is a coefficient that is dependent on which wavelets filtering level is being selected. The value of ξ is dependent on the wavelet filtering level, and the ξ values obtained are listed in Table 1.

Table 1. Values of the Coefficient ξ

wavelets level	ξ
1	2
2	4/3
3	8/7
4	16/15
5	32/31
6	64/63
7	128/127
8	256/255

The elements of the covariance matrix $\mathbf{Q}$ in eq 16 are taken as the variance of the wavelet-filter output, designated as $s_{\hat{Y}_i}^{\ 2}$, which can be roughly estimated by making use of eq 5 as follows:

$$s_{\hat{Y}_i}^{\ 2} = \Lambda_{j*}(k,:)\Lambda_{j*}^\mathrm{T}(k,:)s_{Y_i}^{\ 2} \tag{19}$$

Matrix $\mathbf{Q}$ is assumed to have the following diagonal matrix form:

$$\mathbf{Q} = \mathrm{diag}[s_{\hat{Y}_1}^{\ 2}\ s_{\hat{Y}_2}^{\ 2} \cdots] \tag{20}$$

A guess of the initial state (i.e., $\hat{X}_0$) and a guess of error covariance matrix (P_0) are required to start the estimations at the beginning. $\hat{X}_0$ can use the initial wavelet filtering outputs, and P_0 can be set as $\mathbf{Q}$ in the augmented Kalman filter system.

3.2. Detection and Isolation of Single Gross Error. Single gross error that result from measurement bias or process leaks is considered here. Because the measurement outputs in the Kalman filter estimation are replaced by the wavelet filtering outputs, any abrupt or constant change caused by gross error will be smeared. As a result, the instantaneous residuals from the minimum variance estimation may not be significant for the detection of constant or biased gross errors. Nevertheless, whenever a gross error occurs in some of the state variables, the normality assumptions of the residuals may have been violated. An examination of the history of these residuals can help to investigate the abnormal situations. Besides, an integra-

tion of the constraints to form long-term-based constraints may disclose these violations to help isolate the source of the error. Thus, the gross error detection methodology is described as follows. Define r_{Y_i} be the normalized residual from the Kalman filter estimation for Y_i as follows:

$$r_{Y_i} = \frac{\hat{Y}_{i,K} - Y_i}{s_{Y_i}} \tag{21}$$

where $\hat{Y}_{i,K}$ is the estimation value after Kalman filtering for Y_i. The distribution of residual r_{Y_i} for Y_i is assumed normal in the Kalman filter estimation. A χ^2 variable, which is defined based on history of the residuals, is used to detect the occurrence of the gross error. Define a series of r_{Y_i} as follows:

$$\mathbf{r}_{Y_i} = [r_{Y_i,k-I+1} \ \cdots \ r_{Y_i,k-1} \ \ r_{Y_i,k}]^{\mathrm{T}} \tag{22}$$

where the subscript index k represents r_{Y_i} at the current time instant; the other subscript index (I) represents the length of the history sequence. Because $\mathbf{r}_{Y_i}$ has a normal distribution with variance of 1, the χ^2 variable (γ_{Y_i}) is defined in eq 23:

$$\gamma_{Y_i} = \mathbf{r}_{Y_i}^{\mathrm{T}} \mathbf{r}_{Y_i} \tag{23}$$

The gross error is detected by testing the hypothesis $H_{m,1}$ against $H_{m,0}$:

$$\begin{cases} H_{m,0}: \gamma_{Y_i} < \rho_{I,1-\alpha} \\ H_{m,1}: \gamma_{Y_i} \geq \rho_{I,1-\alpha} \end{cases} \tag{24}$$

where ρ is the χ^2 statistical value for I degrees of freedom at the confidence level α. In each case, if no gross error is considered to exist, $H_{m,0}$ holds; otherwise, $H_{m,1}$ holds.

The integrating constraints are obtained by integrating the system dynamic equations over a prescribed length window as follows:

$$\mathbf{x}_a - \mathbf{x}_{a,0} = [A \ \ B]\mathbf{z} \Rightarrow [-I \ \ \mathbf{A} \ \ \mathbf{B}]\begin{bmatrix}\mathbf{x}_a \\ \mathbf{z}\end{bmatrix} + \mathbf{x}_{a,0} = 0 \Rightarrow D_1\begin{bmatrix}\mathbf{x}_a \\ \mathbf{z}\end{bmatrix} + \mathbf{x}_{a,0} = 0 \tag{25}$$

where $\mathbf{z} = [\mathbf{z}_a \ \mathbf{z}_b]^{\mathrm{T}}$, $\mathbf{z}_a = \int \mathbf{x}_a \, \mathrm{d}t$, and $\mathbf{z}_b = \int \mathbf{x}_{\mathrm{b}} \, \mathrm{d}t$. The standard deviation of $\mathbf{z}$ can be estimated according to eq 26 for m integral points.

$$s_{z_{ai}} = \sqrt{m} * s_{x_{a,i}} \tag{26}$$

$$s_{z_{bi}} = \sqrt{m} * s_{x_{b,i}} \tag{27}$$

The variance of the constraints then is estimated as

$$V_1 = D_1 V D_1^{\mathrm{T}} \tag{28}$$

where V is the variance matrix of the variables $\mathbf{x}_a$ and $\mathbf{z}$:

$$V = \mathrm{diag}([s_{x_{a,i}}^{\ 2} \ \cdots \ s_{z_{a,i}}^{\ 2} \ \cdots \ s_{z_{b,i}}^{\ 2} \ \cdots]) \tag{29}$$

The residual of the constraints (i.e., $\mathbf{v}$) can be obtained in eq 25 as follows:

$$\mathbf{v} = D_1\begin{bmatrix}\hat{\mathbf{x}}_a \\ \hat{\mathbf{z}}\end{bmatrix} + \hat{\mathbf{x}}_{a,0} \tag{30}$$

where $\hat{\mathbf{x}}_a$ is the current Kalman filter state and $\hat{\mathbf{z}}$ is the corresponding time integration. The nodal test is used to examine the normalized $\mathbf{v}$ by V_1 as

$$\kappa_i = \frac{v_i}{V_{1,ii}} \tag{31}$$

The expected value of κ_i is zero; otherwise, gross errors occur in the corresponding constraints. The nodal test uses the following hypotheses:

$$\begin{cases} H_{n,0}: \kappa_i < 3 \\ H_{n,1}: \kappa_i \geq 3 \end{cases} \tag{32}$$

If no gross error in the constraint i is true, $H_{n,0}$ holds; otherwise, $H_{n,1}$ holds.

Combining the two hypothesis tests, the gross error detection and isolation strategy is described as follows:

(1) If $H_{n,1}$ holds for a certain constraint and $H_{m,1}$ holds for variable Y_i ($Y_i \in \mathbf{x}_b$) in this constraint, then a measurement bias of Y_i is diagnosed.

(2) If only $H_{m,1}$ holds for Y_i ($Y_i \in \mathbf{x}_a$), then a measurement bias of Y_i is diagnosed.

(3) If $H_{n,1}$ holds for a certain constraint and $H_{m,1}$ holds for Y_i ($Y_i \in \mathbf{x}_a$), then a process leak in this constraint unit is diagnosed.

4. Example

4.1. Illustration Example of a Four-Tank System. A four-tank system as shown in Figure 6 is illustrated as an example. The system's four differential and algebraic equations are as follows:

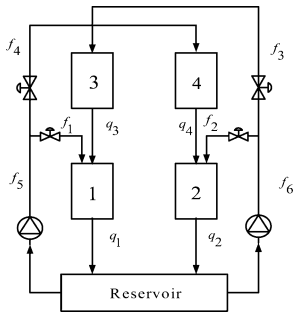

Figure 6. Schematic of a four-tank system.

Table 2. Parameters of the Four-Tank System

symbol	state/parameter	value
h_i	level (cm)	[20.4; 20.4; 11.5; 11.5]
q_i	flow out of the tank i (cm^3/S)	[3; 3; 6;6]
f_i	flow into the tank (cm^3/S)	[3; 3; 3;3; 6; 6]
a_i	area of the drain (cm^2)	[3; 3; 2;2]
g	gravitation constant (cm/S^2)	981
σ_{f}	standard deviation of flow (cm)	0.09
σ_{h}	standard deviation of level (cm)	0.3
A_{r_i}	area of the tanks (cm^2)	1

$$A_{r_1}\frac{\mathrm{d}h_1}{\mathrm{d}t} = -a_1\sqrt{2gh_1} + a_3\sqrt{2gh_3} + f_1 \tag{33a}$$

$$A_{r_2}\frac{\mathrm{d}h_2}{\mathrm{d}t} = -a_2\sqrt{2gh_2} + a_4\sqrt{2gh_4} + f_2 \tag{33b}$$

$$A_{r_3}\frac{\mathrm{d}h_3}{\mathrm{d}t} = -a_3\sqrt{2gh_3} + f_3 \tag{33c}$$

$$A_{r_4}\frac{\mathrm{d}h_4}{\mathrm{d}t} = -a_4\sqrt{2gh_4} + f_4 \tag{33d}$$

Steady-state values and the default measurement noises of the flows and levels in the process are listed in Table 2. Assume

Table 3. Comparisons of the Standardized MSE Values

	MSE	
parameter	by filtered data	by raw data
h_1	0.050	0.492
h_2	0.153	0.491
h_3	0.207	0.607
h_4	0.056	0.79
q_1	0.043	0.302
q_2	0.063	0.291
q_3	0.036	0.270
q_4	0.038	0.259
f_1	0.019	0.221
f_2	0.051	0.269
f_3	0.027	0.307
f_4	0.044	0.258
f_5	0.087	0.299
f_6	0.209	0.299

that all the tank levels and flows are measured and must be reconciled. The system model can be described using the following differential equations:

$$A_{r_1}\frac{dh_1}{dt} = -q_1 + q_3 + f_1 \tag{34a}$$

$$A_{r_2}\frac{dh_2}{dt} = -q_2 + q_4 + f_2 \tag{34b}$$

$$A_{r_3}\frac{dh_3}{dt} = -q_3 + f_3 \tag{34c}$$

$$A_{r_4}\frac{dh_4}{dt} = -q_4 + f_4 \tag{34d}$$

Equality constraints for material balances in this system that should be considered are

$$f_5 = f_1 + f_4 \tag{35a}$$

$$f_6 = f_2 + f_3 \tag{35b}$$

In the first filtering step, the "Daubechies 6" wavelet is selected and a moving-data window with a length equal to 36 is assigned. The length of translations for robust wavelet filtering is 12. The guess of the initial state (i.e., $\hat{X}_0$) is obtained by first calculating the wavelets' filtered values. The guesses of the covariance matrix (P_0 and $\mathbf{Q}$) are set as described. The standardized MSE values (as defined in eq 36) for all the variables are evaluated.

$$\mathrm{MSE} = \frac{1}{N}\sum_{i=1}^{N}\left(\frac{\hat{Y}_{i,K} - Y_i^t}{s_d^t}\right)^2 \tag{36}$$

where $\hat{Y}_{i,K}$ is the estimation value after Kalman filtering for Y_i in each of the moving-data windows, Y_i^t is the corresponding true value, and s_d^t is the standard deviation set in the simulation. N is the total number of points collected in a simulation. Table 3 shows that the reconciliation results are superior to the approaches that use raw measurements. The performances are illustrated in Figures 7, 8, and 9 for h_2, q_2, and f_2, respectively.

4.2. Measurement Bias and Process Leak Detection and Isolation. In the following test, the length of $\mathbf{r}_{Y_i}$ in the measurement test is taken as 10. Under this setting, the adopted χ^2 value, with a confidence level of 0.001, is 29.59, and the number of integral points in the nodal test is assumed to be 20.

4.2.1. Case 1. In the first case, assume that q_2 has a measurement bias with a magnitude of 0.3 that occurs 100 s from the beginning. From the test charts, as shown in Figures 10 and 11, we can see only the measurement test of q_2 and the second nodal test exceed the confident limits. Thus, q_2 with fault is identified.

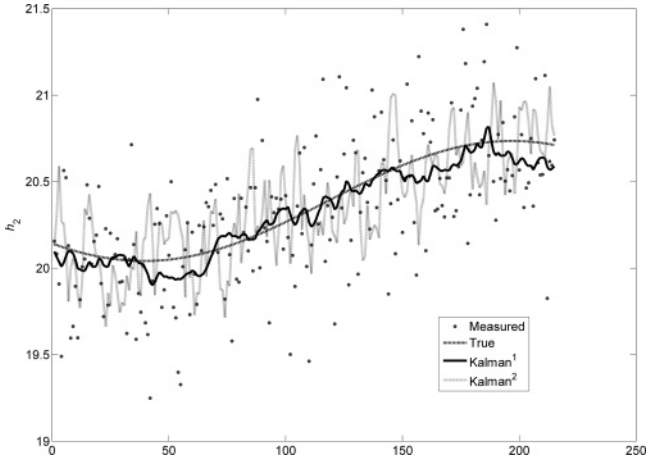

Figure 7. Reconciliation result for variable h_2.

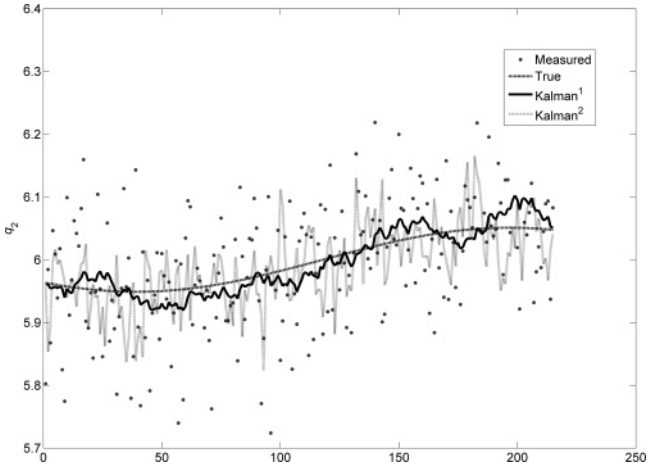

Figure 8. Reconciliation result for variable q_2.

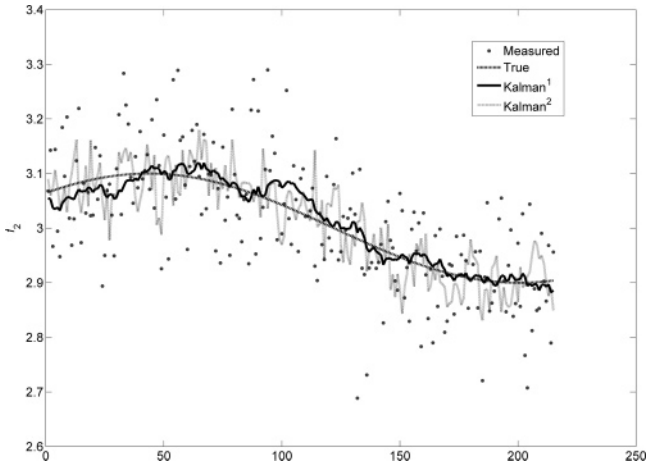

Figure 9. Reconciliation result for variable f_2.

4.2.2. Case 2. Consider a process leak in tank 1 with a magnitude of 0.2 that occurs 15 s from the time origin. The results show that both the statistical value of h_1 and the first constraint exceed their confidence limits, as shown in Figures 12 and 13. Therefore, we conclude that a leak occurs in tank 1.

4.2.3. Case 3. Consider a measurement bias in h_1 with a magnitude of 1 that occurs 100 s from the time origin. We can see that only the measurement test of h_1 exceeds its confident

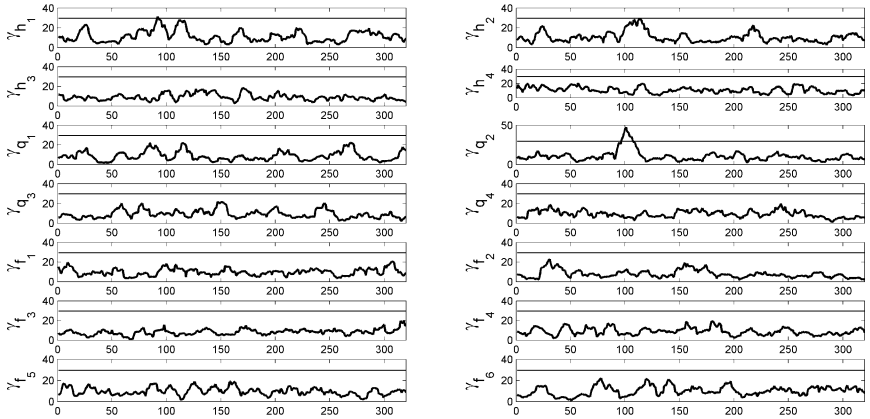

Figure 10. Measurement test for case 1.

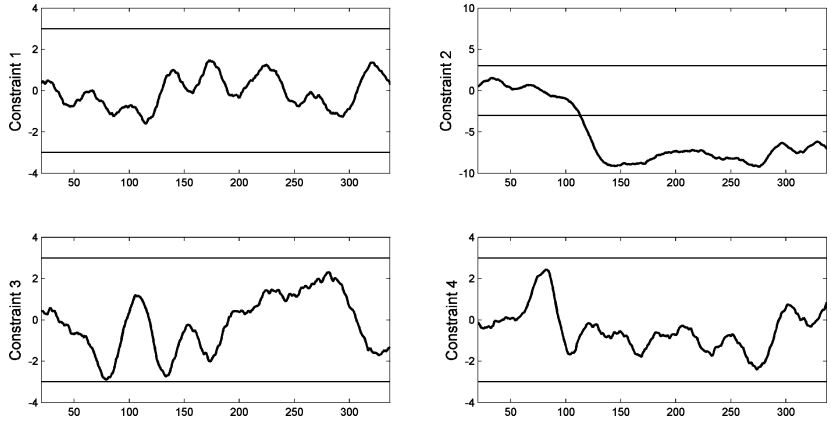

Figure 11. Nodal test for case 1.

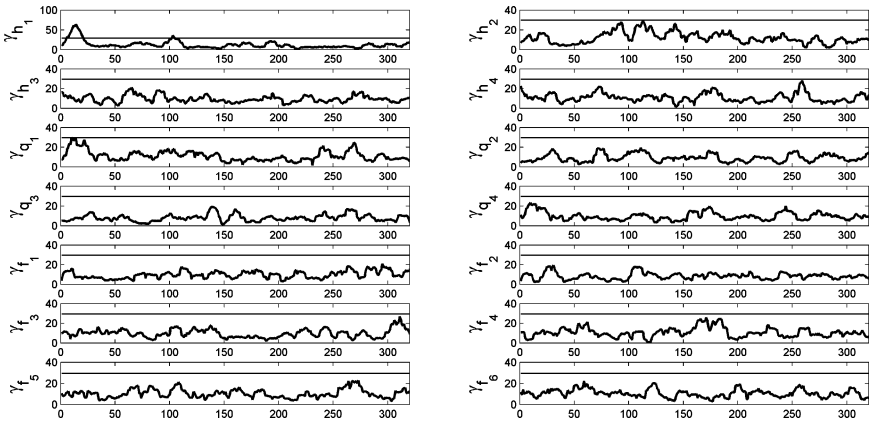

Figure 12. Measurement test for case 2.

level, none in the nodal test, as shown in Figures 14 and 15. Therefore, h_1 with the measurement bias is identified.

5. Conclusions

In this research, an on-line robust filtering method is presented and applied to the dynamic data reconciliation via a Kalman filter approach. By setting the decomposition and reconstruction matrices, simple wavelet filtering can be easily computed. Based on this simple algorithm and the combining uses of the "Translation Invariant" and "Boundary Correction" concepts, the filtering method (which is robust to the effects of outliers) is presented. After the wavelet filtering, most high-frequency noises and outliers are removed. The wavelet-filter outputs then go through a Kalman filter, which takes into account the equality constraints, for the estimations. To ensure that the constraints are being satisfied without biases, accumulative balancing constraints are formulated. From the residuals of each formulated balancing constraints, single gross errors such as constant measurement bias or process leaking flow can be identified. A four-tank linear system is illustrated as an example. The reconciliation performances exhibit significant improvement over those from the un-pretreated data.

Appendix

Matrices $\underline{H}$, $\overline{H}$, $\underline{G}$, and $\overline{G}$ are FIR digital filter arrays, each with a length l. Different wavelets have different such FIR filters and different lengths. The elements of these FIR filters are denoted as $\underline{h}_i$, $\overline{h}_i$, $\underline{g}_i$, and $\overline{g}_i$, respectively. With a given analysis

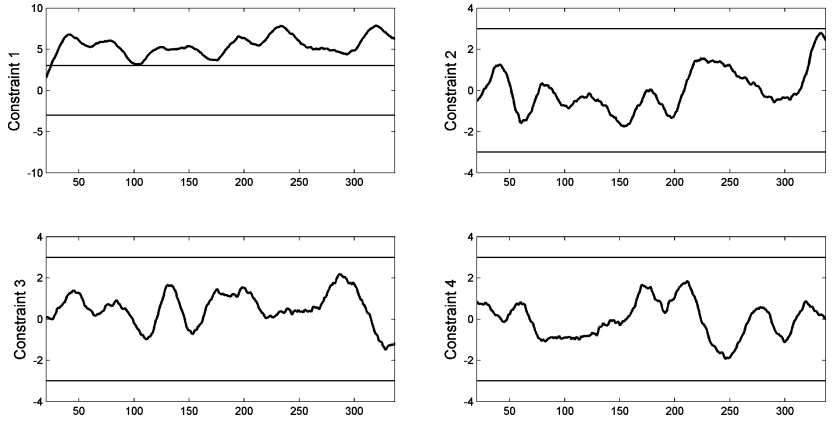

Figure 13. Nodal test for case 2.

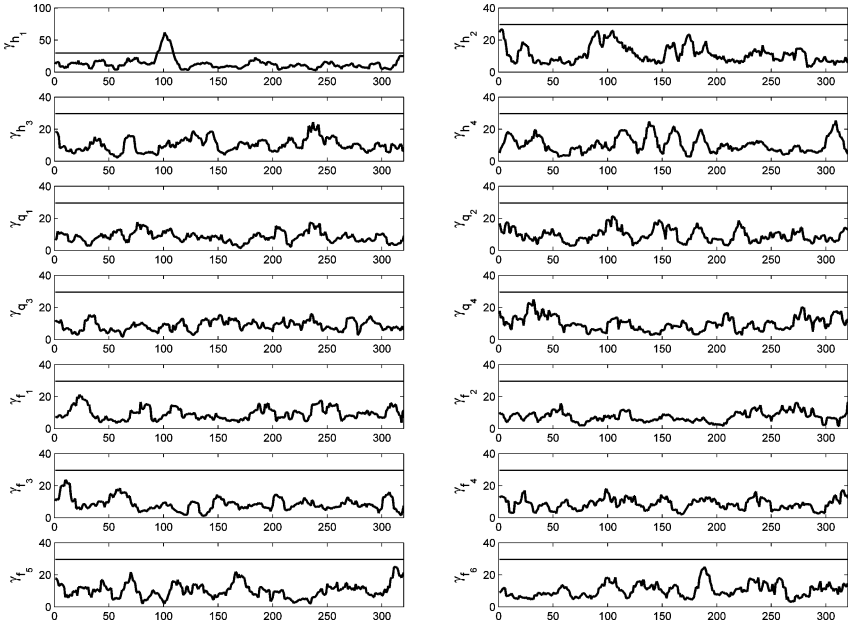

Figure 14. Measurement test for case 3.

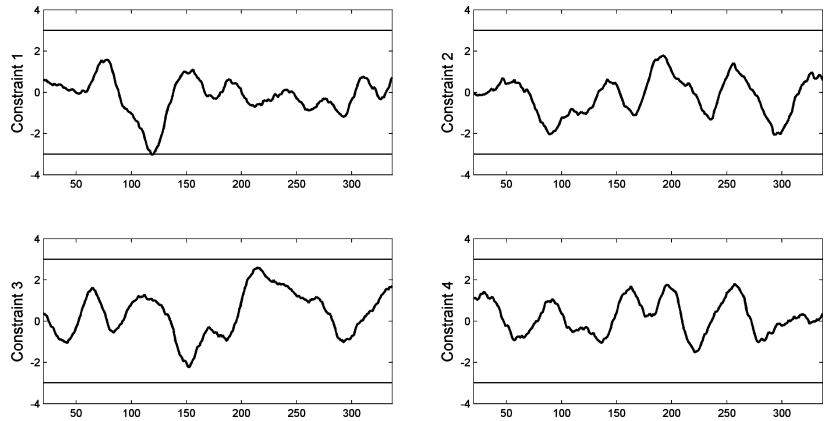

Figure 15. Nodal test for case 3.

level j, in the computation of λ_j from λ_{j-1}, $\underline{\mathbf{T}}_j$ consists of three parts, i.e., $\mathbf{T}_1$, $\mathbf{T}_2$, and $\mathbf{T}_3$, as given in eq 37.

$$\underline{\mathbf{T}}_j = \begin{bmatrix} \mathbf{T}_1 \\ \mathbf{T}_2 \\ \mathbf{T}_3 \end{bmatrix} \tag{37}$$

The structures and dimensions of $\mathbf{T}_1$, $\mathbf{T}_2$, and $\mathbf{T}_3$ are given as follows, where n_j means the length of the coefficients λ_j:

$$\mathbf{T}_1 = \begin{bmatrix} \underline{h}_2 + \cdots + \underline{h}_l & \underline{h}_1 & 0 & \cdots & & & & \\ \underline{h}_4 + \cdots + \underline{h}_l & \underline{h}_3 & \underline{h}_2 & \underline{h}_1 & 0 & \cdots & & \\ \vdots & \vdots & \vdots & \vdots & \ddots & 0 & \cdots & \\ \underline{h}_{l-2} + \cdots + \underline{h}_l & \underline{h}_{l-1} & \cdots & & \underline{h}_2 & \underline{h}_1 & 0 & \cdots \end{bmatrix}_{\left(\frac{l-2}{2}\right)\times(n_{j-1})} \tag{38}$$

$\mathbf{T}_2$ and $\mathbf{T}_3$ have two different forms, depending on whether the length of λ_j is odd or even.

$$\mathbf{T}_2 = \begin{bmatrix} \underline{h}_l & \underline{h}_{l-1} & \underline{h}_{l-2} & \cdots & \underline{h}_2 & \underline{h}_1 & 0 & \cdots & & & & & & \\ & \underline{h}_l & \underline{h}_{l-1} & \cdots & \underline{h}_3 & \underline{h}_2 & \underline{h}_1 & 0 & \cdots & & & & & \\ & & & & & & & \ddots & & & & & & \\ & & & & & & \cdots & 0 & \underline{h}_l & \underline{h}_{l-1} & \underline{h}_{l-2} & \cdots & \underline{h}_2 & \underline{h}_1 \\ & & & & & & & & \cdots & 0 & \underline{h}_l & \underline{h}_{l-1} & \cdots & \underline{h}_3 & \underline{h}_2 & \underline{h}_1 \end{bmatrix}_{\mathrm{E},(n_j-l+2)\times(n_{j-1})} \tag{39}$$

$$\mathbf{T}_2 = \begin{bmatrix} \underline{h}_l & \underline{h}_{l-1} & \underline{h}_{l-2} & \cdots & \underline{h}_2 & \underline{h}_1 & 0 & \cdots & & & & & & \\ & \underline{h}_l & \underline{h}_{l-1} & \cdots & \underline{h}_3 & \underline{h}_2 & \underline{h}_1 & 0 & \cdots & & & & & \\ & & & & & & & \ddots & & & & & & \\ & & & & & & \cdots & 0 & \underline{h}_l & \underline{h}_{l-1} & \underline{h}_{l-2} & \cdots & \underline{h}_2 & \underline{h}_1 \\ & & & & & & & & \cdots & 0 & \underline{h}_l & \underline{h}_{l-1} & \cdots & \underline{h}_3 & \underline{h}_2 & \underline{h}_1 \end{bmatrix}_{\mathrm{O},(n_j-l+1)\times(n_j-1)} \tag{40}$$

$$\mathbf{T}_3 = \begin{bmatrix} \cdots & 0 & \underline{h}_l & \underline{h}_{l-1} & \cdots & & \underline{h}_4 & \underline{h}_1 + \cdots + \underline{h}_3 \\ & & & \ddots & & & \vdots & \\ & & \cdots & 0 & \underline{h}_l & \underline{h}_{l-1} & \underline{h}_{l-2} & \underline{h}_1 + \cdots + \underline{h}_{l-3} \\ & & & \cdots & 0 & \underline{h}_l & \underline{h}_1 + \cdots + \underline{h}_{l-1} & \end{bmatrix}_{\mathrm{E},\left(\frac{l-2}{2}\right)\times(n_{j-1})} \tag{41}$$

$$\mathbf{T}_3 = \begin{bmatrix} \cdots & 0 & \underline{h}_l & \underline{h}_{l-1} & \cdots & & \underline{h}_3 & \underline{h}_1 + \cdots + \underline{h}_2 \\ & & & \ddots & & & \vdots & \\ & & & \cdots & 0 & \underline{h}_l & \underline{h}_{l-1} & \underline{h}_1 + \cdots + \underline{h}_{l-2} \\ & & & & \cdots & 0 & \underline{h}_l & \underline{h}_1 + \cdots + \underline{h}_l \end{bmatrix}_{\mathrm{O},(l/2)\times(n_{j-1})} \tag{42}$$

where the subscripts E and O denote even and odd lengths of λ_j. $\overline{\mathbf{T}}_j$ is obtained from $\underline{\mathbf{T}}_j$ by replacing each $\underline{h}_i$ with $\bar{h}_i$.

Similarly, at a given analysis level j, $\underline{\mathbf{S}}_j$ also has two different forms, according to whether n_j is odd or even. $\underline{\mathbf{S}}_j$ is composed of $\underline{g}_i$, as follows:

$$\underline{\mathbf{S}}_i = \begin{bmatrix} \underline{g}_{l-1} & \underline{g}_{l-3} & \cdots & \underline{g}_3 & \underline{g}_1 & & & & & & & & \\ \underline{g}_l & \underline{g}_{l-2} & \cdots & \underline{g}_4 & \underline{g}_2 & & & & & & & & \\ & \underline{g}_{l-1} & \underline{g}_{l-3} & \cdots & \underline{g}_3 & \underline{g}_1 & & & & & & & \\ & \underline{g}_l & \underline{g}_{l-2} & \cdots & \underline{g}_4 & \underline{g}_2 & & & & & & & \\ & & & & & \ddots & & & & & & & \\ & & & & & & \ddots & & & & & & \\ & & & & & & & \underline{g}_{l-1} & \underline{g}_{l-3} & \cdots & \underline{g}_3 & \underline{g}_1 & \\ & & & & & & & \underline{g}_l & \underline{g}_{l-2} & \cdots & \underline{g}_4 & \underline{g}_2 & \\ & & & & & & & & \underline{g}_{l-1} & \underline{g}_{l-3} & \cdots & \underline{g}_3 & \underline{g}_1 \\ & & & & & & & & \underline{g}_l & \underline{g}_{l-2} & \cdots & \underline{g}_4 & \underline{g}_2 \end{bmatrix}_{\mathrm{E},(n_{j-1})\times(n_j)} \tag{43}$$

$$\underline{\mathbf{S}}_i = \begin{bmatrix} \underline{g}_{f-1} & \underline{g}_{f-3} & \cdots & \underline{g}_3 & \underline{g}_1 & & & & & & & & \\ \underline{g}_f & \underline{g}_{f-2} & \cdots & \underline{g}_4 & \underline{g}_2 & & & & & & & & \\ & \underline{g}_{f-1} & \underline{g}_{f-3} & \cdots & \underline{g}_3 & \underline{g}_1 & & & & & & & \\ & \underline{g}_f & \underline{g}_{f-2} & \cdots & \underline{g}_4 & \underline{g}_2 & & & & & & & \\ & & & & & \ddots & & & & & & & \\ & & & & & & \ddots & & & & & & \\ & & & & & & & \underline{g}_{f-1} & \underline{g}_{f-3} & \cdots & \underline{g}_3 & \underline{g}_1 & \\ & & & & & & & \underline{g}_f & \underline{g}_{f-2} & \cdots & \underline{g}_4 & \underline{g}_2 & \\ & & & & & & & & \underline{g}_{f-1} & \underline{g}_{f-3} & \cdots & \underline{g}_3 & \underline{g}_1 \end{bmatrix}_{\mathrm{O},(n_{j-1})\times(n_j)} \tag{44}$$

$\overline{\mathbf{S}}_j$ is obtained from $\underline{\mathbf{S}}_j$ by replacing each $\underline{g}_i$ with $\bar{g}_i$.

Nomenclature

a_i = area of the drain
a_t = colored noise input
$\mathbf{A}$ = system matrix of the Kalman filter approach
A_{r_i} = area of the tank i
$\mathbf{B}$ = system input matrix of the Kalman filter approach
c = Student t-statistical value for level determination
$\mathbf{c}$ = set of wavelet coefficients

$\mathbf{C}_a$, $\mathbf{C}_b$ = measurement matrix of the system
$\mathbf{d}$ = constant term of the equality constraint
$\mathbf{d}^{(j)}$ = residuals of the measurements and the jth level filtered signal
$\bar{\mathbf{d}}^{(j)}$ = mean of $\mathbf{d}^{(j)}$
$\mathbf{D}$ = state equality constraint matrix
e_t = colored noise output
$\mathbf{e}$ = measurement noises of the system
f_i = flow i into the tank
g = gravitation constant
$\underline{G}$ = the low-pass filter for reconstruction
$\overline{G}$ = the high-pass filter for reconstruction
h_i = level of tank i
$\underline{H}$ = the low-pass filter for decomposition
$\overline{H}$ = the high-pass filter for decomposition
j = wavelet analysis level
k = the length of the wavelets filtering window
P = state error covariance
$\mathbf{Q}_a$ = covariance matrix of $\mathbf{w}_a$
$\mathbf{Q}_b$ = covariance matrix of $\mathbf{w}_b$
q_i = flow i out of the tank
r_{Y_i} = normalized residual from Kalman filter estimation
$\mathbf{r}_{Y_i}$ = time series of r_{Y_i}
R = covariance matrix of $\mathbf{e}$
$s_{x_{a,i}}$ = standard deviation of $x_{a,i}$
$s_{z_{a,i}}$ = standard deviation of $z_{a,i}$
$s_{z_{b,i}}$ = standard deviation of $z_{b,i}$
$s_{\mathrm{d}}^{(j)}$ = standard deviation of $\mathbf{d}^{(j)}$
s_{Y_i} = standard deviation of Y_i
$s_{\hat{Y}_i}$ = standard deviation of the wavelets filtered signal
$\underline{\mathbf{S}}_j$ = reconstruction matrix for approximate coefficients at level j
$t^{(j)}$ = Student t-statistical value
$\mathbf{T}_a$ = discrete wavelet analysis matrix
$\mathbf{T}_s$ = inverse discrete wavelet analysis matrix
$\underline{\mathbf{T}}_j$ = decomposition matrix for approximate coefficients at level j
$\mathbf{v}$ = residual of the constraint
V = covariance matrix of the constraint
V_1 = covariance matrix of the integral variables
$\mathbf{w}_a$, $\mathbf{w}_b$ = system disturbance
$\mathbf{x}_a$ = set of state variables
$\mathbf{x}_b$ = set of state variables
X = augmented state variable of the Kalman filter approach
$y_k^{(j)}$ = the last filtered point in the data window
Y_i = measurement of variable Y_i
$\hat{Y}_{i,K}$ = estimation of Kalman filter for variable Y_i
$\mathbf{y}$ = data window of the measurements
$\mathbf{y}^{(j)}$ = reconstructed signal from the low-pass coefficients at level j
$\mathbf{Y}$ = measurements of the Kalman filter approach
$\mathbf{z} = \mathbf{z} = [\mathbf{z}_a\ \mathbf{z}_b]^{\mathrm{T}}$, where $\mathbf{z}_a = \int \mathbf{x}_a\, \mathrm{d}t$ and $\mathbf{z}_b = \int \mathbf{x}_b\, \mathrm{d}t$

Greek Letters

$\gamma_{Y_i} = \mathbf{r}_{Y_i}^{\mathrm{T}} \mathbf{r}_{Y_i}$
$\rho = \chi^2$ statistical value for gross error detection
$\eta = \chi^2$ statistical value for level determination
ξ = coefficient for standard deviation
κ_i = normalized residual of the constraint
$\chi^{2,(j)}$ = chi-squared statistical value of $\mathbf{d}^{(j)}$
σ_{f} = standard deviation of flow
σ_{h} = standard deviation of tank level
$\lambda^{(j)}$ = the set of jth level wavelet function coefficients
Λ_j = the wavelet filter matrix of level j

Literature Cited

(1) Stanley, G. M.; Mah, R. S. H. Estimation of Flow and Temperatures in Process Networks. *AIChE J.* **1977**, *23*, 642−650.

(2) Darouach, M.; Ragot, J.; Fayolle, J.; Maquin, D. Data Validation in Large-scale Steady-state Linear Systems. Presented at the World Congress on Scientific Computation, Paris, France, 1988.

(3) Almasy, G. A. Principles of Dynamic Balancing. *AIChE J.* **1990**, *36*, 1321−1330.

(4) Becerra, V. M.; Roberts, P. D.; Griffiths, G. W. Dynamic Data Reconciliation for Sequential Modular Simulators: Application to a Mixing Process. *Proc. Am. Control Conf.* **2000**, *4*, 2740−2744.

(5) Vachhani, P.; Rengaswamy, R.; Gangwal, V.; Narasimhen, S. Recursive Estimation in Constrained Nonlinear Dynamical Systems. *AIChE J.* **2005**, *51*, 946−959.

(6) Narasimhan, S.; Jordache, C. *Data Reconciliation and Gross Error Detection—An Intelligent Use of Process Data*; Gulf Publishing Company: Houston, TX, 2000.

(7) Porrill, J. Optimal Combination and Constraints for Geometrical Sensor Data. *Int. J. Robot. Res.* **1988**, *7*, 66−77.

(8) Hayward, S. Constrained Kalman Filter for Least-squares Estimation of Time-varying Beamforming Weights. In *Mathematics in Signal Processing IV*; McWhirter, J., Proudler, I., Eds.; Oxford University Press: New York, 1998; pp 113−125.

(9) Simon, D.; Chia, T. L. Kalman Filtering with State Constraints. *IEEE Trans. Aerosp. Electron. Syst.* **2002**, *38*, 128−136.

(10) Heinonen, P.; Neuvo, Y. FIR-Median Hybrid Filters. *IEEE Trans. Aroust. Speech Signal Process.* **1987**, *35*, 832−838.

(11) Mallat, S. G. A Theory for Multiresolution Signal Decomposition: The Wavelet Representation. *IEEE Trans. Pattern Anal. Mach. Intell.* **1989**, *11*, 674−693.

(12) Donoho, D. L. Nonlinear Wavelet Methods for Recovering Signals, Images, and Densities from Indirect and Noisy Data. *Proc. Symp. Appl. Math.* **1993**, 173−205.

(13) Donoho, D. L. De-noising by Soft-Thresholding. *IEEE Trans. Inf. Theory* **1995**, *41*, 613−627.

(14) Donoho, D. L.; Johnstone, I. M.; Kerkyacharian, G.; Picard, D. Wavelets Shrinkage: Asymptotia? *J. R. Stat. Soc. B* **1995**, *57*, 301−369.

(15) Coifman, R. R.; Donoho, D. L. Translation Invariant De-noising. *Lect. Notes Statist.: Wavelets Stat.* **1995**, *103*, 125−150.

(16) Mallat, S.; Zhong, S. Characterization of Signals from Multiscale Edges. *IEEE Trans. Pattern Anal. Mach. Intell.* **1992**, *14*, 710−732.

(17) Jensen, A.; Cour-Harbo, A. *Ripples in Mathematics—The Discrete Wavelet Transform*; Springer−Verlag: Berlin, Heidelberg, 2001.

(18) Nounou, M. N.; Bakshi, B. R. Online Multiscale Filtering for Random and Gross Errors without Process Models. *AIChE J.* **1999**, *45*, 1041−1058.

(19) Bruce, A. G.; Donoho, D. L.; Gao, H. Y.; Martin, R. D. Denoising and Robust Nonlinear Wavelet Analysis. *SPIE Proc., Wavelet Appl.* **1994**, *2242*, 325−336.

(20) Doymaz, F.; Bakhtazad, A.; Romagnoli, J. A.; Palazoglu, A. Wavelet-based Robust Filtering of Process Data. *Comput. Chem. Eng.* **2001**, *25*, 1549−1559.

(21) Luo, K.; Huang, H. A Wavelet Enhanced Integral Approach to Linear Dynamic Data Reconciliation. *J. Chem. Eng. Jpn.* **2005**, *38*, 1035−1048.

(22) Grewal, M. S.; Andrews, A. P. *Kalman Filtering: Theory and Practice Using MATLAB*; Wiley: New York, 2001.

Received for review November 3, 2006
Revised manuscript received September 3, 2007
Accepted September 5, 2007

IE061410K